ELSEVIER

Biochimica et Biophysica Acta 1553 (2002) 84–101

BIOCHIMICA ET BIOPHYSICA ACTA

BBA

www.bba-direct.com

Review

Succinate:quinone oxidoreductases from ε-proteobacteria[1]

C. Roy D. Lancaster [a,*], Jörg Simon [b]

[a] *Max Planck Institute of Biophysics, Department of Molecular Membrane Biology, Heinrich-Hoffmann-Str. 7, D-60528 Frankfurt am Main, Germany*

[b] *Institute of Microbiology, Johann Wolfgang Goethe University, Marie-Curie-Str. 9, D-60439 Frankfurt am Main, Germany*

Received 20 June 2001; received in revised form 21 September 2001; accepted 12 October 2001

Abstract

The ε-proteobacteria form a subdivision of the Proteobacteria including the genera *Wolinella*, *Campylobacter*, *Helicobacter*, *Sulfurospirillum*, *Arcobacter* and *Dehalospirillum*. The majority of these bacteria are oxidase-positive microaerophiles indicating an electron transport chain with molecular oxygen as terminal electron acceptor. However, numerous members of the ε-proteobacteria also grow in the absence of oxygen. The common presence of menaquinone and fumarate reduction activity suggests anaerobic fumarate respiration which was demonstrated for the rumen bacterium *Wolinella succinogenes* as well as for *Sulfurospirillum deleyianum*, *Campylobacter fetus, Campylobacter rectus* and *Dehalospirillum multivorans*. To date, complete genome sequences of *Helicobacter pylori* and *Campylobacter jejuni* are available. These bacteria and *W. succinogenes* contain the genes *frdC*, *A* and *B* encoding highly similar heterotrimeric enzyme complexes belonging to the family of succinate:quinone oxidoreductases. The crystal structure of the *W. succinogenes* quinol:fumarate reductase complex (FrdCAB) was solved recently, thus providing a model of succinate:quinone oxidoreductases from ε-proteobacteria. Succinate:quinone oxidoreductases are being discussed as possible therapeutic targets in the treatment of several pathogenic ε-proteobacteria.

Keywords: Fumarate reductase; Fumarate respiration; Succinate dehydrogenase; *Wolinella succinogenes*; *Helicobacter pylori*; *Campylobacter jejuni*

1. Introduction

The Proteobacteria are divided into five subdivisions (α, β, γ, δ, and ε) based on 16S rRNA gene sequence similarity. The ε-subdivision comprises the Campylobacteraceae (genera *Campylobacter*, *Arcobacter*, *Sulfurospirillum*), the Helicobacteraceae (genera *Helicobacter*, *Wolinella*, *Thiovolum*, *Flexispira*) and the genus *Dehalospirillum* [1–6].

Campylobacter spp. are either commensals or pathogens that colonise the mucosal surfaces of the intestinal tracts, oral cavities, or urogenital tracts of a wide range of bird and animal hosts. *C. jejuni* is the leading cause of bacterial food-borne diarrhoeal disease throughout the world [7]. The best known species of *Helicobacter*, *H. pylori*, inhabits the gastric mucosa of the human stomach and is recognised as the major aetiological factor in chronic gastritis, peptic ulcer disease, and as a risk factor for gastric cancer (see [8,9] for recent reviews). The genera *Wolinella* and *Dehalospirillum* each comprise only one

* Corresponding author. http://www.mpibp-frankfurt.mpg.de/lancaster.

E-mail address: roy.lancaster@mpibp-frankfurt.mpg.de (C.R.D. Lancaster).

[1] Dedicated to Achim Kröger on the occasion of his 65th birthday

0005-2728/02/$ – see front matter
PII: S0005-2728(01)00230-4

species: *W. succinogenes* was isolated from bovine rumen [4,13] whereas *D. multivorans* is a free-living bacterium isolated from activated sludge [5]. Species of the genus *Sulfurospirillum* were isolated from anoxic or microoxic aquatic habitats [6,10,11]. Cells of *W. succinogenes*, *D. multivorans* and *Sulfurospirillum deleyianum* can be proliferated in defined minimal media in contrast to *Helicobacter* spp. and *Campylobacter* spp. which grow only in complex media.

Although all members of the ε-proteobacteria are closely related phylogenetically there is a high variability in energy metabolism (Table 1). Most ε-proteobacteria are oxidase-positive microaerophiles which grow best in the presence of 2–10% (v/v) O_2 and 3–10% (v/v) CO_2. Under these conditions, an oxygen-reducing terminal oxidase is required which is usually a CO-binding cytochrome complex. *W. succinogenes* is an exception, since a rather low rate of formate oxidation by oxygen was reported [12] and no CO-binding cytochromes were detected. Nevertheless, *W. succinogenes* was reported to reduce oxygen and to grow microaerobically in the presence of 2% oxygen with concomitant formation of H_2O_2 [6,13]. However, cells of *W. succinogenes* grow considerably faster anaerobically by fumarate or nitrate respiration than in the presence of oxygen. Further species of ε-proteobacteria do also grow under anoxic conditions, e.g. species of the genera *Campylobacter* and *Sulfurospirillum* (Table 1) whereas *D. multivorans* was described as strictly anaerobic. In the absence of oxygen, a terminal oxidase is dispensable and the bacteria have to rely on other sources of ATP, e.g. anaerobic respiration using alternative electron acceptors (Table 1). Growth by fumarate respiration was demonstrated for *W. succinogenes* [14], *D. multivorans* [5], *S. deleyianum* [6], *Campylobacter fetus* [15] and *Campylobacter rectus* [16,17]. The enzymology and energetics of *W. succinogenes* fumarate respiration are reviewed elsewhere in this issue [14]. Since the majority of the ε-proteobacteria was found to contain only menaquinones (menaquinone-6 (MK-6) and methylmenaquinone-6 (MMK-6)) and to reduce fumarate to succinate, fumarate respiration might be a commonality within this bacterial subdivision.

Here we compare the properties of succinate:quinone oxidoreductases and their possible metabolic roles in ε-proteobacteria in the context of the three-

Table 1
Properties of representative ε-proteobacteria during aerobic and anaerobic growth (data compiled from references [1–4,6,12,16,17,60,75–79])

Organism	Microaerophilic growth	Anaerobic growth	Type of terminal oxidase	CO-binding cytochrome	Catalase present	Electron acceptors of anaerobic respiration [a]	Major quinone(s)
W. succinogenes	+	+	n.r.	–[b]	–	Fumarate, polysulphide, NO_3^-, NO_2^-, DMSO	MK-6, MMK-6
H. pylori	+	–	cbb_3 [c]	+	+	–	MK-6
C. jejuni	+	–	cbb_3, *bd*[c]	+	+	–	MK-6, MMK-6
C. rectus	+	+	*cb*-type	+	–	Fumarate	n.r.
S. deleyianum	+	+	n.r.	n.r.	–	Fumarate, NO_3^-, NO_2^-, DMSO, S^0, SO_3^{2-}, $S_2O_3^{2-}$	MK-6, MMK-6

n.r.: property not reported.
[a]Growth demonstrated using H_2 or formate as electron donor.
[b]Cells grown anaerobically with fumarate as acceptor.
[c]Predicted by the genome sequence.

dimensional structure of *W. succinogenes* quinol:fumarate reductase (QFR) [18]. A more general view on the physiology and metabolic properties of *H. pylori* is given in [19–22]. Complete genome sequences are available for two independent isolates of *H. pylori* [23,24] and for *C. jejuni* [25].

2. Role of succinate:quinone oxidoreductases in energy metabolism

Succinate:quinone oxidoreductases are generally assumed to be membrane-bound and similar in subunit composition and amino acid sequence. These enzymes can be functionally divided into QFRs and succinate:quinone reductases (SQR) [26]. Both types of enzymes are known to catalyse fumarate reduction as well as succinate oxidation [27], and it is not possible to determine their in vivo function by simply comparing the respective amino acid sequences.

In aerobic organisms, SQRs catalyse the oxidation of succinate by ubiquinone (reaction (1)). The oxidation of ubiquinol with O_2 (reaction (2)) is then coupled to the translocation of protons from the 'inside' (cytoplasmic or matrix) space (H_i^+) to the 'outside' (periplasmic or intermembrane) space (H_o^+) generating an electrochemical proton potential (Δp) across the membrane that drives ADP phosphorylation according to the chemiosmotic mechanism [28].

$$\text{Succinate} + \text{Q} \rightarrow \text{Fumarate} + \text{QH}_2 \quad (1)$$

$$\text{QH}_2 + 0.5\ \text{O}_2 + n\ \text{H}_i^+ \rightarrow \text{Q} + \text{H}_2\text{O} + n\ \text{H}_o^+ \quad (2)$$

Succinate oxidation with menaquinone is energetically unfavourable. In *Bacillus subtilis*, an aerobic bacterium that contains only menaquinone, succinate oxidation is therefore thought to be driven by the Δp (reaction (3)) [29,30] which in turn is generated by O_2-dependent oxidation of menaquinol (reaction (4)). A similar mechanism can be expected for the conversion of succinate to fumarate in aerobic ε-proteobacteria.

$$\text{Succinate} + \text{MK} + n\ \text{H}_o^+ \rightarrow \text{Fumarate} + \text{MKH}_2 + n\ \text{H}_i^+ \quad (3)$$

$$\text{MKH}_2 + 0.5\ \text{O}_2 + n\ \text{H}_i^+ \rightarrow \text{MK} + \text{H}_2\text{O} + n\ \text{H}_o^+ \quad (4)$$

The SQR of *B. subtilis* is similar to the QFR involved in *W. succinogenes* fumarate respiration. In this case, the Δp is generated by oxidation of H_2 or formate by fumarate (reactions (5) and (6)) [14].

$$\text{H}_2 + \text{Fumarate} + n\ \text{H}_i^+ \rightarrow \text{Succinate} + n\ \text{H}_o^+ \quad (5)$$

$$\text{HCO}_2^- + \text{H}^+ + \text{Fumarate} + n\ \text{H}_i^+ \rightarrow \text{CO}_2 + \text{Succinate} + n\ \text{H}_o^+ \quad (6)$$

The process of fumarate respiration is a widespread property of numerous anaerobic and facultatively anaerobic bacteria [14,31]. Fumarate respiration in *W. succinogenes* was demonstrated with cells growing in a minimal medium with formate or H_2 as electron donor and fumarate as terminal acceptor and sole carbon source [14,31,32]. Oxidation of hydrogen or formate cannot serve in ATP synthesis by substrate level phosphorylation. Instead, menaquinone is reduced by hydrogenase or formate dehydrogenase in a process assumed to be coupled to the apparent translocation of one proton per electron across the membrane by a so-called redox loop mechanism (reactions (7) and (8)) [14,33]. Menaquinol is oxidised by the membrane-bound QFR (reaction (9)). There are conflicting experimental results as to whether this process contributes to Δp generation (discussed in [14] and below).

$$\text{H}_2 + \text{MK} + 2\ \text{H}_i^+ \rightarrow \text{MKH}_2 + 2\ \text{H}_o^+ \quad (7)$$

$$\text{HCO}_2^- + \text{H}_o^+ + \text{MK} + 2\ \text{H}_i^+ \rightarrow \text{CO}_2 + \text{MKH}_2 + 2\ \text{H}_o^+ \quad (8)$$

$$\text{MKH}_2 + \text{Fumarate} + 2\ \text{H}_i^+ \rightarrow \text{MK} + \text{Succinate} + 2\ \text{H}_{o/i?}^+ \quad (9)$$

The presence of menaquinone and a succinate:quinone oxidoreductase (see Section 3) suggests the occurrence of fumarate respiration in *H. pylori* and *C. jejuni*. However, the occurrence of this process is difficult to prove with growing cells because of the complex nutritional requirements of these bacteria. To the knowledge of the authors, anaerobic growth of *H. pylori* or *C. jejuni* with fumarate as electron acceptor was not reported (Table 1). The genomes of *H. pylori* and *C. jejuni* both contain genes (*hydA*, *B*

Table 2
Amino acid sequence identities (%) of succinate:quinone oxidoreductases from ε-proteobacteria compared to the A, B, and C subunits of *W. succinogenes* QFR

Organism	FrdA	FrdB	FrdC	Ref.
H. pylori NCTC11639	66 (455/684)	71 (168/236)	58 (143/243)	[41]
H. pylori 26695	67 (463/683)	70 (167/236)	58 (141/243)	[23]
H. pylori J99	67 (461/683)	70 (167/236)	58 (143/243)	[24]
C. jejuni	69 (459/660)	68 (162/237)	53 (125/233)	[25]

The first and second numbers in parentheses refer to the absolute number of identical residues and to the length of the aligned sequence.

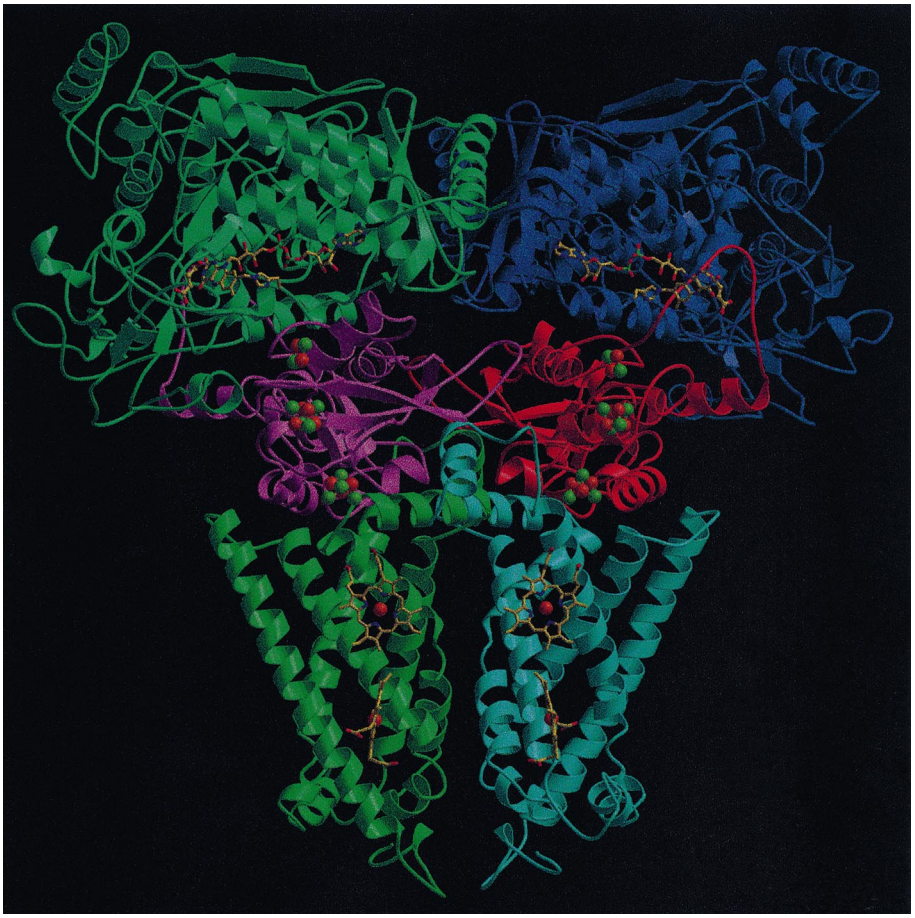

Fig. 1. Three-dimensional structure of the *W. succinogenes* QFR dimer of heterotrimeric complexes of A, B, and C subunits. The Cα traces of the two A subunits are shown in blue and blue-green, those of the two B subunits in red and purple and those of the two C subunits in green and light blue. The atomic structures of the six prosthetic groups per heterotrimer are superimposed for better visibility. From top to bottom, these are the covalently bound FAD, the [2Fe–2S], the [4Fe–4S], and the [3Fe–4S] iron–sulphur centres, the proximal and the distal haem *b* groups. Atomic colour coding is as follows: C, N, O, P, S, and Fe are displayed in yellow, blue, red, light green, green, and orange, respectively. The figure is drawn from the PDB coordinate set 1QLA [18]. The position of bound fumarate close to the isoalloxazine ring of FAD is taken from the coordinate set 1QLB [18]. Figs. 1, 2, 4–6 were prepared with a version of Molscript [81] modified for colour ramping [82] capabilities. In addition, this figure was prepared with the program Raster3D [83].

Fig. 2. Subunit A, the flavoprotein of *W. succinogenes* QFR (stereo views). (a) The Cα trace of subunit A is drawn in blue (FAD-binding domain), green (capping domain), purple and pink (helical domain), and orange/yellow (C-terminal domain). Drawn as atomic models is the side chain of Arg A301 of the capping domain at the active site, and the FAD group which is covalently bound to His A43 of the FAD-binding domain. The amino-terminus is at the bottom of the panel in the middle, the carboxy-terminus on the right. (b and c) Main chain traces of *W. succinogenes* QFR subunit A, colour-coded according to sequence conservation with the succinate:quinone oxidoreductases from *H. pylori* and *C. jejuni* (cf. Table 2). Drawn in green is the main chain of those residues which are either identical or share Ser/Thr homology. All other residues are indicated by a red main chain. (b) Trace drawn for residues A1–409. The histidyl-FAD and the Arg A301 side chain are included as atomic models to facilitate orientation. (c) Trace drawn for residues A410–655.

→

and *C*) that predict subunits of a membrane-bound hydrogenase similar to that of *W. succinogenes* [34]. A *W. succinogenes*-like formate dehydrogenase operon [35,36] was found in the genome of *C. jejuni*, but not in *H. pylori*. The specific activity of fumarate reduction measured as the production rate of succinate was increased eight-fold to 24 U g protein^{-1} upon the addition of formate (5 mM) to whole cell suspensions of *C. jejuni* [37]. The observed correlation between the production of succinate and the disappearance of formate suggests an electron transport chain from formate to fumarate. Alternatively the FrdCAB complex may function as a SQR during microaerobic growth of *Helicobacter* spp. and *Campylobacter* spp. as discussed in Section 6.

3. Genes and gene products

The QFR of *W. succinogenes* is a membrane-bound heterotrimeric complex that consists of the subunits FrdA (73 kDa), FrdB (27 kDa) and FrdC (30 kDa) [18]. The catalytic subunit FrdA contains covalently bound FAD near the active site. FrdB ligates three iron–sulphur clusters. The hydrophobic protein FrdC is a dihaem cytochrome *b* membrane anchor that is required for naphthoquinol oxidation (cf. Section 4). The genes encoding the subunits of the *W. succinogenes* QFR were cloned and sequenced [38,39]. The consecutive open reading frames designated *frdC*, *A*, and *B* were found to be co-transcribed in *W. succinogenes* [40]. Ge et al. [41] sequenced similar open reading frames cloned from the genome of *H. pylori* strain NCTC11639 and the same arrangement was found by genome sequencing of *H. pylori* strain 26695 [23] and strain J99 [24]. From the known genome sequences it was concluded that *H. pylori* does not contain a further succinate:quinone oxidoreductase. The genome sequence of *C. jejuni* revealed similar *frdC*, *A*, and *B* genes in the same order. The predicted FrdA, FrdB, and FrdC proteins from *H. pylori* and *C. jejuni* share a high degree of identical residues with those of *W. succinogenes* (Table 2). Three additional open reading frames of the *C. jejuni* genome were annotated as *sdhA*, *B* and *C* that might encode a SQR. The predicted sequence of *C. jejuni* SdhC is not similar to those of the FrdC proteins. This protein rather belongs to a family with similarity to SdhC from *Sulfolobus acidocaldarius* and *Acidianus ambivalens* and to heterodisulphide reductase subunit B of methanogenic Archaea [42–46].

4. Structure of the *W. succinogenes* QFR

Three structures of the *W. succinogenes* QFR complex are now available, based on three different crystal forms [18,47,48], all of the monoclinic space group $P2_1$ (see [49] for a recent review on the crystallisation of *W. succinogenes* QFR). In all three crystal forms, two heterotrimeric complexes of A, B, and C subunits are associated in an identical fashion, thus forming the dimer shown in Fig. 1. As derived from analytical gel filtration experiments, this dimer is apparently also present in the detergent-solubilised state of the enzyme [50], implying that it is unlikely to be an artifact of crystallisation.

4.1. The flavoprotein subunit A and the mechanism of fumarate reduction/succinate oxidation

The structure obtained from the first crystal form of *W. succinogenes* QFR, 'A', which has the unit cell dimensions $a = 85.2$ Å, $b = 189.0$ Å, $c = 117.9$ Å, and $\beta = 104.5°$, was refined at 2.2 Å resolution (PDB entry 1QLA [18]). It shows that subunit A is composed

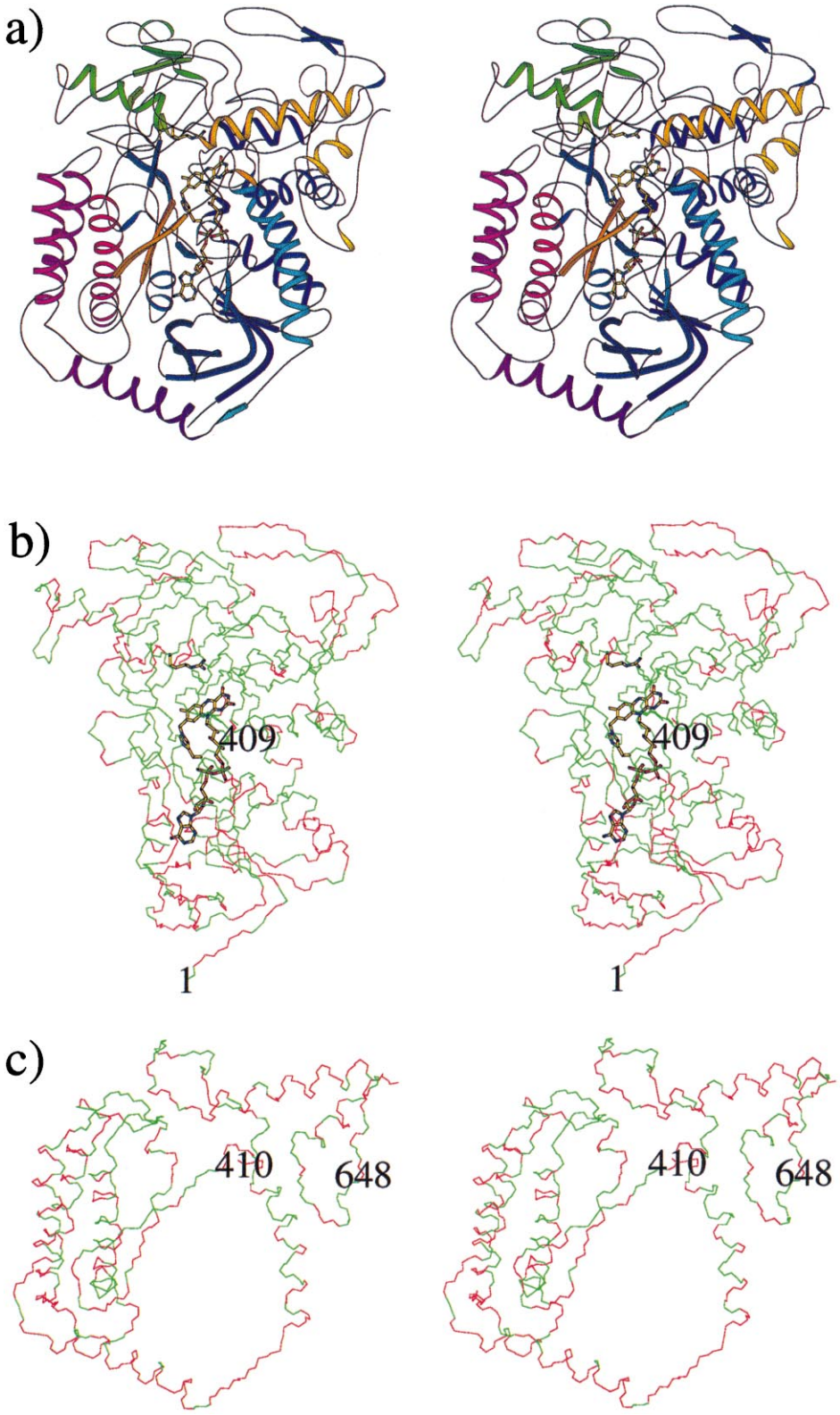
a)
b)
409
1
409
1
c)
410
648
410
648

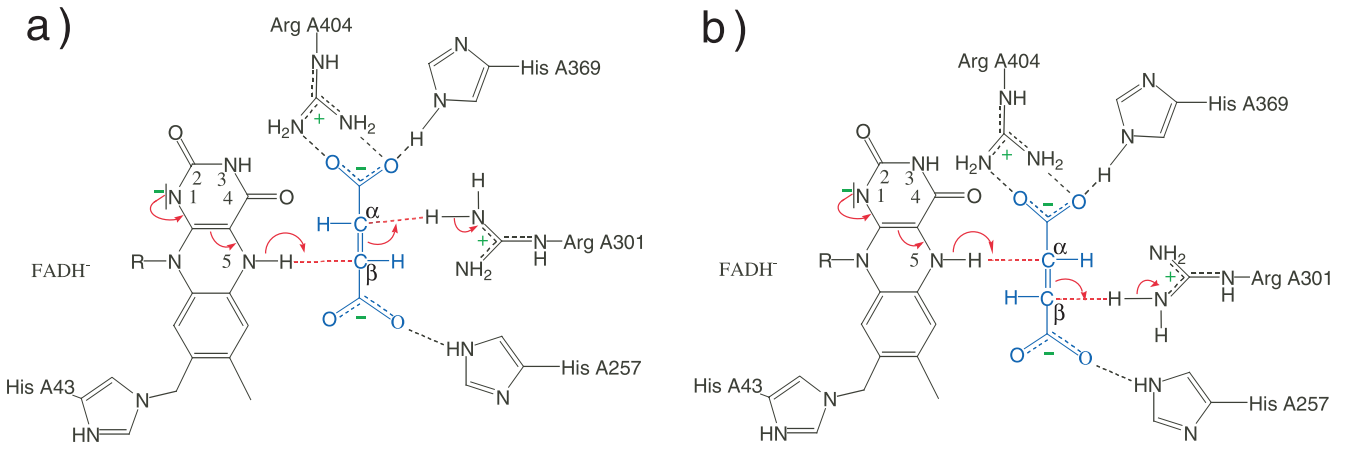

Fig. 3. (a and b) Alternative possible mechanisms of fumarate reduction in *W. succinogenes* QFR derived from the structure in crystal form C. Since the precise location of the bound fumarate molecule in this crystal form is not yet known, it could be either the β-methenyl group (a) or the α-methenyl group (b) which is reduced by hydride transfer from the N5 position of $FADH^-$. This is coupled to proton transfer to the respective other methenyl group from the side chain of Arg A301. From [48] (a) and [52] (b).

of four domains (see Fig. 2a), the bipartite FAD-binding domain (blue, residues A1–260 and A366–436, with 'A' indicating the A subunit), into which the capping domain (green, A260–366) is inserted, the helical domain (purple and pink, A436–554), and the C-terminal domain (orange and yellow, A554–655). The FAD is covalently bound as 8α-[*N*ε-histidyl]-FAD [51] to the residue His A43. The capping domain contributes to burying the otherwise solvent-exposed FAD isoalloxazine ring from the protein surface.

A *W. succinogenes* QFR crystal grown in the presence of fumarate was found to be of crystal form 'B' with unit cell dimensions of $a = 118.4$ Å, $b = 85.1$ Å, $c = 188.9$ Å, and $\beta = 96.5°$. The structure was refined at 2.33 Å resolution (PDB entry 1QLB [18]). This allowed the localisation of the fumarate-binding site between the FAD-binding domain and the capping domain next to the plane of the FAD isoalloxazine ring.

The structure of the enzyme in the third crystal form, 'C' with unit cell dimensions $a = 81.1$ Å, $b = 290.2$ Å, $c = 153.6$ Å, and $\beta = 95.7°$ [47], was refined at 3.1 Å resolution (PDB entry 1E7P [48]). Compared with the previous crystal forms, the capping domain is rotated in this structure relative to the FAD-binding domain. This leads to interdomain closure at the fumarate-reducing site, suggesting that the structure encountered in this crystal form represents a closer approximation to the catalytically competent state of the enzyme. The *trans* hydrogenation of fumarate to succinate could occur by the combination of the transfer of a hydride ion and of a proton from opposite sides of the fumarate molecule. One of the fumarate methenyl carbon atoms could be reduced by direct hydride transfer from the N5 position of the reduced $FADH^-$, while the other fumarate methenyl carbon is protonated by the side chain of Arg A301 (see Fig. 3a,b) [48]. The latter residue replaces the water molecule previously suggested to be the proton donor [18] based on the structure in crystal form B. As pointed out earlier [52], the assignment as to which of the fumarate methenyl carbon atoms accepts the hydride and which the proton is currently ambiguous (Fig. 3a versus Fig. 3b), because data of sufficient completeness and quality for this crystal form have so far only been obtained for the complex with malonate and

→

Fig. 4. Subunit B, the iron–sulphur protein of *W. succinogenes* QFR. (a) The Cα trace of subunit B is drawn in blue (amino-terminal [2Fe–2S] domain, residues B1–106) and orange/pink/purple (carboxy-terminal [7Fe–8S] domain, B106–239). From top left to bottom right, the iron–sulphur clusters are [2Fe–2S], [4Fe–4S], [3Fe–4S]. The Cys ligands of the iron–sulphur clusters are labelled by their residue number. (b) (stereo view) Main chain traces of *W. succinogenes* QFR subunit B. Colour coding according to sequence conservation among the succinate:quinone oxidoreductases from ε-proteobacteria is as for Fig. 2b,c.

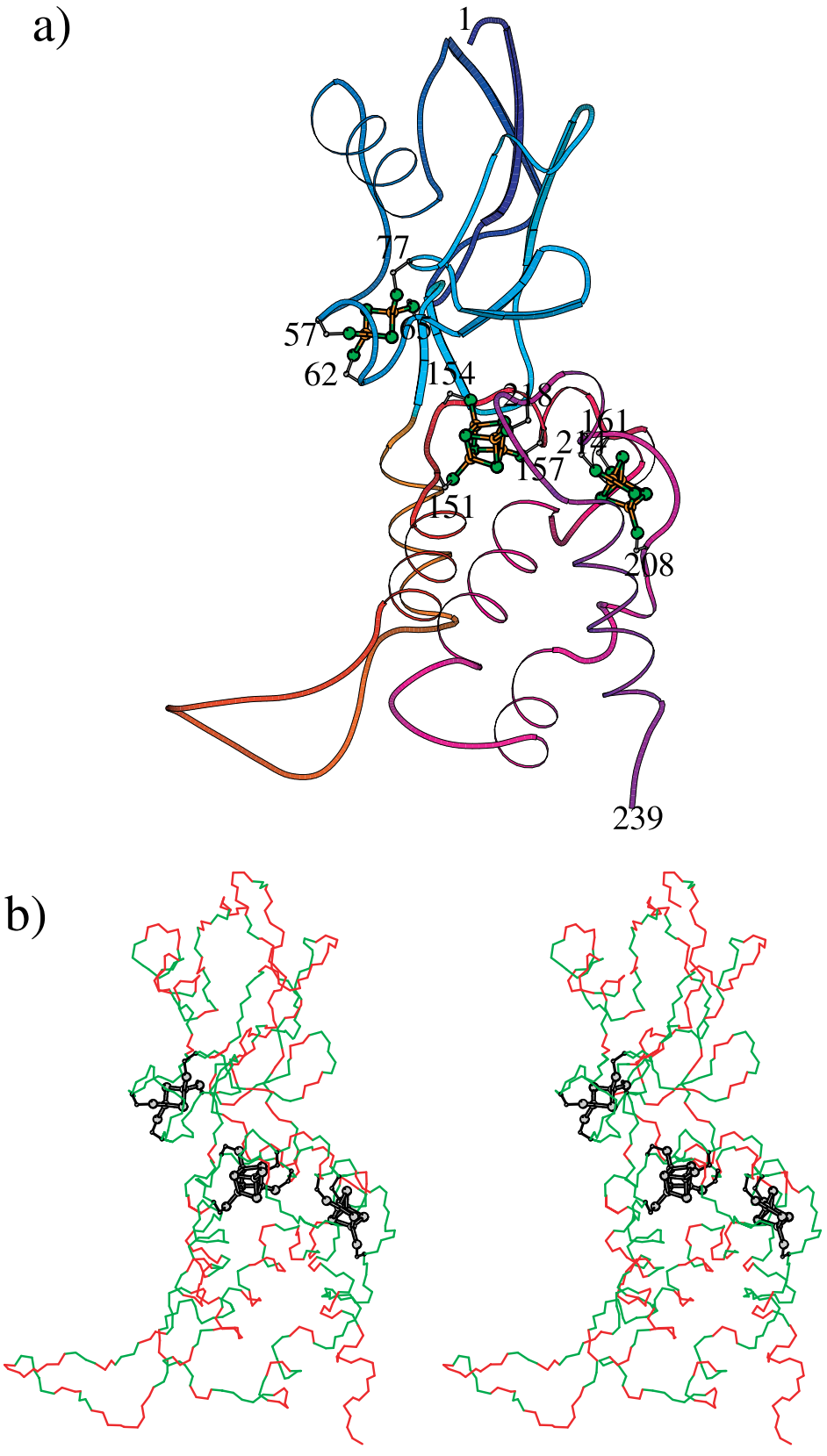
a)
1
77
57
62
154
218
161
214
157
151
208
239
b)

not yet in the presence of fumarate. Release of the product could be facilitated by movement of the capping domain away from the dicarboxylate site [18,48]. All residues implicated in substrate binding and catalysis are conserved throughout the superfamily of succinate:quinone oxidoreductases, so that this reversible mechanism is considered generally relevant for all succinate:quinone oxidoreductases.

Not surprisingly, residues of *W. succinogenes* QFR subunit A conserved among the succinate:quinone oxidoreductases from ε-proteobacteria (cf. Table 2) are predominantly found in the internal regions of the FAD-binding domain and the capping domain, as indicated by a green main chain trace in Fig. 2b,c. However, there is also considerable conservation in the second half of the C-terminal domain, a region of unknown function which is not conserved in succinate:quinone oxidoreductases from other species.

4.2. Subunit B, the iron–sulphur protein

The Cα trace of *W. succinogenes* subunit B is shown in Fig. 4. This subunit of 27 kDa [39] consists of two domains (see Fig. 4a), an N-terminal 'plant ferredoxin' domain (B1–106), binding the [2Fe–2S] iron–sulphur centre and a C-terminal 'bacterial ferredoxin' domain (B106–239) binding the [4Fe–4S] and the [3Fe–4S] iron–sulphur centres. The [2Fe–2S] iron–sulphur centre is coordinated by the Cys residues B57, B62, B65 and B77 as predicted on the basis of sequence alignments [39]. All four Cys residues are within segments that are in contact with the A subunit. The [4Fe–4S] iron–sulphur centre is ligated to the protein through Cys residues B151, B154, B157 and B218, and the [3Fe–4S] centre is coordinated by Cys residues B161, B208 and B214. The latter three residues are within segments that are in contact with the C subunit. Residues of *W. succinogenes* QFR subunit B which are conserved among the succinate:quinone oxidoreductases from ε-proteobacteria (cf. Fig. 4b) are concentrated around the iron–sulphur centres and the adjacent regions of contact with the A and C subunits, respectively.

4.3. Subunit C, the dihaem cytochrome b

The Cα trace of *W. succinogenes* subunit C is shown in Fig. 5. This subunit of 30 kDa [38] contains five membrane-spanning segments with preferentially helical secondary structure. These segments are labelled (according to [53]) I (residues C22–52, blue in Fig. 5a), II (C77–100, blue-green), IV (C121–149, yellow), V (C169–194, red), and VI (C202–237, pink). According to the sequence alignment in [53] and the structural alignment in [18], there is no transmembrane segment III in the *W. succinogenes* QFR. To varying degrees, all five transmembrane segments are tilted with respect to the membrane normal, and helix IV is strongly kinked at position C137. This kink is stabilised by the side chain γ-hydroxyl of Ser C141, which is conserved in the enzymes from ε-proteobacteria and which, instead of its backbone NH, donates a hydrogen bond to the carbonyl oxygen of Phe C137 [50]. As pointed out earlier [50], this feature is very similar to that found for helix F of bacteriorhodopsin (bR, PDB entry 1C3W [54], Fig. 3b), part of which tilts during the bR photocycle [55]. The membrane-spanning segments are connected by four loops, three of which contain short helices (pI–II, light blue in Fig. 5a; cII–IV: green; pIV–V: orange, with 'p' and 'c' indicating segments on the periplasmic and cytoplasmic sides, respectively). The N-terminus of subunit C is on the cytoplasmic, the C-terminus on the periplasmic side of the membrane. The N-terminal residues C3–11 form a helix denoted 'cN' (dark blue).

The planes of both haem molecules bound by the *W. succinogenes* enzyme are approximately perpen-

→

Fig. 5. Subunit C, the dihaem cytochrome *b* of *W. succinogenes* QFR (stereo views). Also shown are the proximal (upper) and distal (lower) haem groups and the position of the [3Fe–4S] cluster (top), which is bound by the B subunit (see Fig. 4). Selected C subunit residues are labelled by their residue number. (a) The Cα trace of subunit C is drawn in dark blue (amino-terminus), blue (transmembrane helix I), light blue (periplasmic I–II connection), blue-green (transmembrane helix II), green (cytoplasmic II–IV connection), yellow (transmembrane helix IV), orange (periplasmic IV–V connection), red (transmembrane helix V), pink (transmembrane helix VI), and purple (carboxy-terminus). (b) Main chain traces of *W. succinogenes* QFR subunit C. Colour coding according to sequence conservation among the succinate:quinone oxidoreductases from ε-proteobacteria is as for Fig. 2b,c.

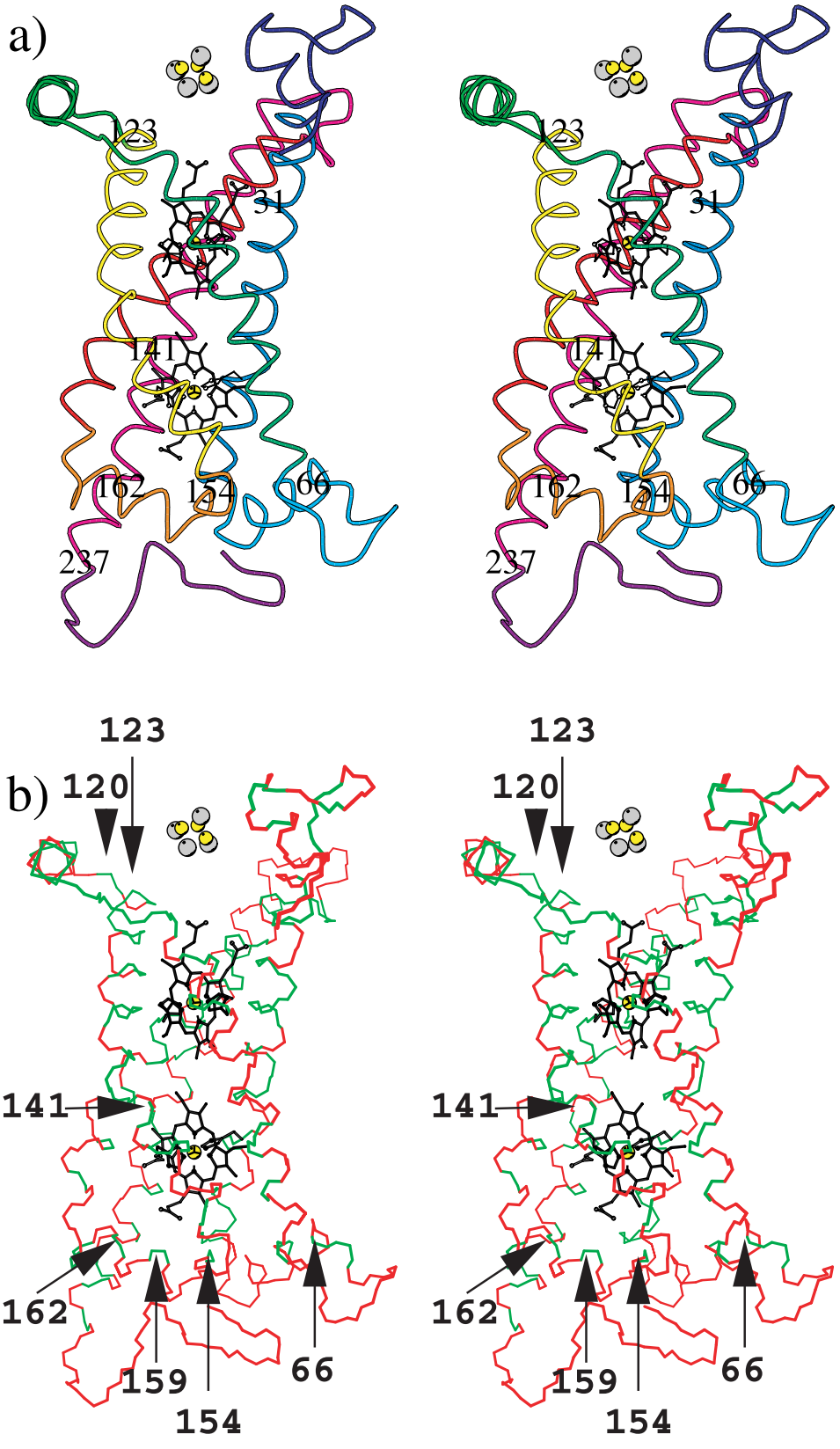
a)
123
31
141
162
154
66
237
123
31
141
162
154
66
237
b)
123
120
141
162
159
154
66
123
120
141
162
159
154
66

dicular to the membrane surface and their interplanar angle is 95° [18]. The axial ligands to the 'proximal' haem b_P are His C93 of transmembrane segment II and His C182 of transmembrane segment V (Fig. 6a). This causes haem b_P to be located towards the cytoplasmic surface of the membrane, and thus towards the [3Fe–4S] iron–sulphur centre. Hydrogen bonds and salt bridges with the propionate groups of haem b_P are formed with the side chains of residues Gln C30, Ser C31, Trp C126 and Lys C193 [18] (see Fig. 6a). Thus, side chains from the residues of the first four transmembrane segments are involved in the binding of haem b_P, which underscores the structural importance of the bound haem [40]. The axial ligands to the 'distal' haem b_D are His C44 of transmembrane segment I and His C143 of transmembrane segment IV [18] (see Fig. 6b), demonstrating that all four haem axial ligands had been correctly predicted by sequence alignment [38] and site-directed mutagenesis [40].

As noted earlier [18], the binding of the two haem *b* groups described here is very different from that described for the cytochrome bc_1 complex [56]. In *W. succinogenes* QFR, the axial ligands for haem binding are located on four different transmembrane segments. In the cytochrome bc_1 complex, only two transmembrane segments are involved, each providing two axial haem *b* ligands. One consequence of this difference is that the distance between the two haem iron centres is distinctly shorter in QFR (15.6 Å) than it is in the cytochrome bc_1 complex (21 Å).

Residues of *W. succinogenes* QFR subunit C conserved among the succinate:quinone oxidoreductases from ε-proteobacteria (see Fig. 5b) are concentrated around the haem groups and the contact surface with subunit B (e.g. His C120, Thr C123, Trp C126, see Fig. 6a). However, a distal 'rim' of conserved residues is also apparent, involving residues Glu C66, Ile C154, Ser C159 and Arg C162 (see Fig. 6b). While the latter two residues interact with a propionate of haem b_D, Glu C66 and Ile C154 are likely to play a role in the binding of the menaquinol substrate, as discussed below.

4.4. The site of menaquinol oxidation/menaquinone reduction

The site of MKH_2 oxidation on the dihaem cytochrome *b* subunit of *W. succinogenes* QFR is not known. No density for a quinol or quinone could be found in any of the three crystal forms of the oxidised enzyme. No specific inhibitor of MKH_2 oxidation by *W. succinogenes* QFR has been identified. In the crystal structure, a cavity which extends from the hydrophobic phase of the membrane, close to the distal haem b_D, to the periplasmic aqueous phase could accommodate a MKH_2 molecule, after minor structural alterations [47] which are consistent with experimentally observed structural differences for the presence and absence of a quinone substrate [57]. A glutamate residue (Glu C66) lines the cavity and could accept a hydrogen bond from one of the hydroxyl groups of MKH_2 (Fig. 6b).

Replacement of Glu C66 by a glutamine residue resulted in a variant enzyme which did not catalyse quinol oxidation by fumarate, whereas the subunit C-independent activity of succinate oxidation by methylene blue was not affected [47]. X-ray crystal structure analysis of the Glu C66→Gln variant enzyme ruled out significant structural alterations and the midpoint potentials of the two haem groups of subunit C were virtually unaffected. These results indicate that the inhibition of quinol oxidation activity in the mutant enzyme is due to absence of the carboxyl group of Glu C66. Thus it was concluded that Glu C66, which is conserved in the enzymes from the ε-proteobacteria *C. jejuni* and *H. pylori* (see Fig. 6b), is an essential constituent of the menaquinol oxidation site [47] close to haem b_D (Fig. 6b).

→

Fig. 6. Conserved proximal (a) and distal (b) residues in the structure of *W. succinogenes* QFR (stereo views). The Cα trace of subunit C is colour-coded as described for Fig. 5a. (a) In addition to the Cα trace of subunit C, that of subunit B is shown in black. Also indicated are two conserved B subunit residues (B209 and B216). All other labelling refers to selected proximal C subunit residues. The following prosthetic groups are included from the top left to the bottom right: the [4Fe–4S] cluster, the [3Fe–4S] cluster, the proximal haem and the distal haem. (b) Selected distal C subunit residues are labelled. The proximal (upper) and distal (lower) haem are included as is the tentative menaquinol-binding position suggested in [47]. Transmembrane helices II and VI have been omitted for clarity.

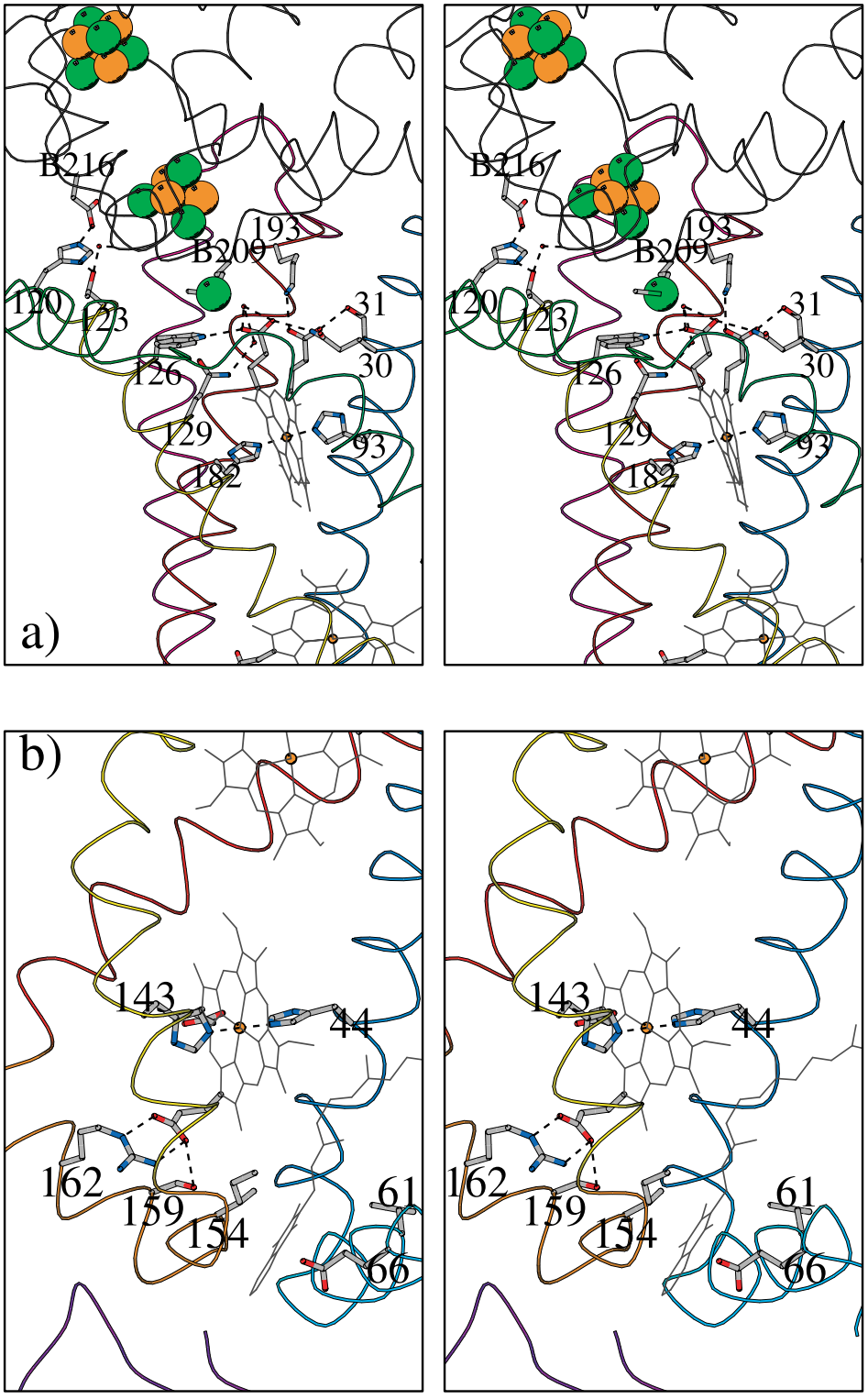
B216
193
B209
120
123
31
126
30
129
93
182
a)
b)
143
44
162
159
154
61
66

4.5. Electron and proton transfer

For the function of QFR, electrons have to be transferred from the quinol-oxidising site in the membrane to the fumarate-reducing site, protruding into the cytoplasm. For *W. succinogenes* QFR, the experimental data [58] are consistent with this electron transfer from the quinol to fumarate occurring via (at least) one haem *b* group. The very short distance between haem b_P and haem b_D strongly suggests a role in electron transfer for both haem *b* groups, as does the localisation of the menaquinol oxidation site close to Glu C66.

The arrangement of the prosthetic groups in the QFR dimer is displayed in Figs. 1 and 7. The fumarate molecule is in van der Waals contact with the isoalloxazine ring of FAD. Fig. 7 also includes the edge-to-edge distances between the prosthetic groups as defined by Page and coworkers [59]. Distances shorter than 14 Å, i.e. within one QFR heterotrimer but not between the two heterotrimers of the dimer, are considered to be short enough to support physiological electron transfer. The edge-to-edge distance between the tentative menaquinol model and haem b_D is 6.7 Å. The linear arrangement of the six prosthetic groups of one heterotrimeric QFR complex shown in Fig. 7 therefore provides one straightforward possible pathway by which electrons could be transferred efficiently from the menaquinol oxidation site via the dihaem cytochrome *b*, the three iron–

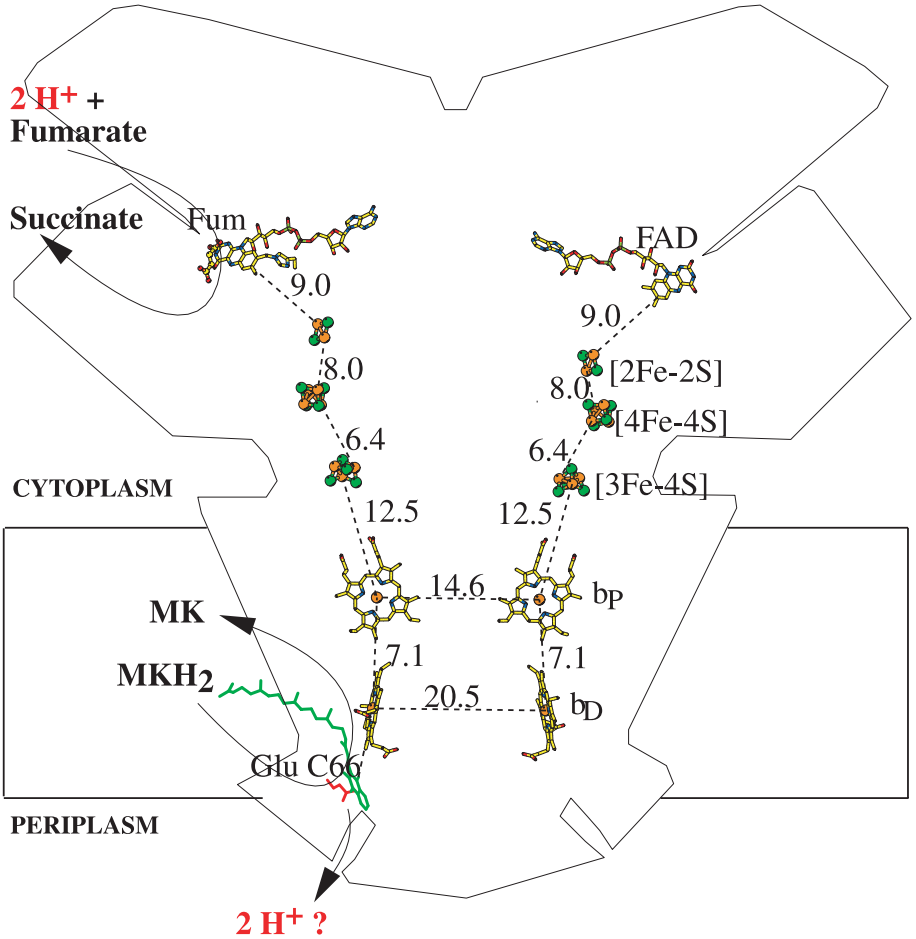

Fig. 7. The prosthetic groups of the *W. succinogenes* QFR dimer are displayed (coordinate set 1QLA [18]). Distances between prosthetic groups are edge-to-edge distances in Å as defined in [59]. Also drawn is the side chain of Glu C66, which has been shown to be essential for menaquinol oxidation [47]. The tentative model of menaquinol binding (drawn in green) is taken from [47]. The position of bound fumarate (Fum) is taken from PDB entry 1QLB [18]. The direction of proton release upon quinol oxidation is hypothetical. See text for details.

sulphur centres and the FAD to the dicarboxylate-binding site.

The two haem groups have different oxidation–reduction potentials [60], one is the 'high-potential' haem b_H ($E_M = -20$ mV or -15 mV for the membrane-bound [60] and detergent-solubilised [47] QFR enzyme, respectively), the other the 'low-potential' haem b_L ($E_M = -200$ mV [60] and -150 mV [47], respectively). It has not yet been established which of the haems b_P and b_D corresponds to b_L and b_H in *W. succinogenes* QFR.

The redox midpoint potentials of the iron–sulphur centres [58] follow the order high (-24 mV)–low (< -250 mV)–high (-59 mV) with increasing proximity to the covalently bound FAD. The [4Fe–4S] iron–sulphur centre has a very low potential ($E_M < -250$ mV) and has been suggested not to participate in electron transfer (see [26] for a review). However, the determined low potential may be an artefact due to anti-co-operative electrostatic interactions between the redox centres [61]. The position of the [4Fe–4S] centre as revealed in the structure of *W. succinogenes* QFR is highly suggestive of its direct role in electron transfer from the [3Fe–4S] centre to the [2Fe–2S] centre. Despite this major thermodynamically unfavourable step, the calculated rate of electron transfer is on a microsecond scale, demonstrating that this barrier can easily be overcome by thermal activation as long as the electron transfer chain components are sufficiently close to promote intrinsically rapid electron tunnelling [62].

In addition to the transfer of electrons, two protons are bound upon fumarate reduction and two protons are liberated upon menaquinol oxidation (see Eq. 9 and Fig. 7). The protons consumed upon fumarate reduction are bound from the cytoplasm. The experimental results on intact bacteria, with inverted vesicles or liposomes containing *W. succinogenes* QFR discussed by Kröger et al. [14], suggest that the oxidation of MKH_2 by fumarate as catalysed by *W. succinogenes* QFR is an electroneutral process. The protons formed by MKH_2 oxidation have therefore been assumed to be released to the cytoplasmic side of the membrane where they balance the protons consumed by fumarate reduction [14,50].

However, the essential role of Glu C66 for menaquinol oxidation demonstrated in [47] contrasts this interpretation. Most probably, this residue acts by accepting a proton formed by MKH_2 oxidation. Since there is no obvious structural indication of a proton channel within the C subunit which would guide the protons formed in MKH_2 oxidation to the cytoplasmic side of the membrane, it is difficult to envisage proton release on the cytoplasmic side of the membrane as required for electroneutrality. Instead, as depicted schematically in Fig. 7, release of the protons to the periplasm is strongly suggested by this location of the menaquinol oxidation site. In summary, the location of the catalytic sites of fumarate reduction and menaquinol oxidation in the structure indicates that quinol oxidation by fumarate is an electrogenic process in *W. succinogenes*, in full agreement with results for *B. subtilis* SQR (see Eq. 3) in the direction of both succinate oxidation [29] and fumarate reduction [30] (see also [52] for a discussion), but in contrast to the presently available results of experimental measurements for *W. succinogenes* QFR [14]. Currently, we have no satisfactory explanation for this discrepancy. However, we cannot rule out the possibility that the quinol oxidation process is coupled to the transfer of protons to the cytoplasm through a proton transfer pathway which is transiently established during the catalytic cycle of the enzyme and is not obvious from the available crystal structure of the oxidised enzyme. This would be consistent with both a distal quinol oxidation site and the observed apparent electroneutrality. We are currently investigating this possibility further.

5. Enzymatic properties

The QFR of *W. succinogenes* is the best characterised succinate:quinone oxidoreductase of an ε-proteobacterium and is the only such enzyme for which quinone reactivity has been shown [14,27]. The Michaelis constant (K_M) for fumarate determined with various electron donors was 0.35 mM [63]. The K_M value for succinate measured with methylene blue or menadione as electron acceptor was 7 mM and 20 mM, respectively, indicating that the *W. succinogenes* enzyme predominantly functions in the direction of fumarate reduction. The activity of QFRs can be determined using different assays (reviewed in [64]) that make use of either: (1) the oxidation of succi-

Table 3
Specific activities of fumarate reduction and succinate oxidation in cell lysates (CL) or membrane fractions (MF) of ε-proteobacteria

	Succinate oxidation (U mg protein^{-1})		Fumarate reduction (U mg protein^{-1})		
			by benzyl viologen		by $DMNH_2$
	CL	MF	CL	MF	CL
W. succinogenes[a]	1.4[b]	2.7[b]	14	27	1.1
H. pylori	0.02[c]	0.06[b]	n.r.	0.78/0.48[d]	n.r.

One unit of activity corresponds to the conversion of 1 μmol succinate or fumarate min^{-1} mg protein^{-1}. n.r.: not reported.
[a]Data from [80].
[b]Determined with methylene blue as acceptor.
[c]Determined with either methylene blue or 2,6-dichlorophenolindophenol and phenazine methosulphate as acceptor [65,66].
[d]Data from two different strains [41].

nate to fumarate by methylene blue, (2) the reduction of fumarate to succinate by reduced viologen dyes or (3) the reduction of fumarate to succinate by 2-3-dimethyl-1,4-naphthoquinol ($DMNH_2$). Specific activities for the enzyme from *W. succinogenes* are given in Table 3.

Birkholz et al. [65] purified the fumarate-reducing enzyme from the membrane fraction of *H. pylori*. The proteins FrdA (80 kDa) and FrdB (31 kDa) were identified by cross-reaction with antisera raised against the corresponding subunits of *W. succinogenes* fumarate reductase. Fumarate reductase activity in *H. pylori* was only found in the membrane fraction [41,65]. The specific activity of succinate oxidation by methylene blue was 0.02 U mg protein^{-1} in the cell lysate (Table 3). A similar specific succinate dehydrogenase activity was measured in a *H. pylori* cell lysate using 2,6-dichlorophenolindophenol and phenazine methosulphate as electron acceptor [66]. The activity was in the same range as that of fumarate reduction with NADH as electron donor. Assuming that there is only one succinate:quinone oxidoreductase in *H. pylori*, these results indicate that this enzyme catalyses succinate oxidation as well as fumarate reduction. Ge et al. [41] reported a fumarate reduction activity of 0.78 U mg protein^{-1} and 0.48 U mg protein^{-1} in the respective membrane fractions of two *H. pylori* strains using benzyl viologen radical as donor substrate. The corresponding activity of the *W. succinogenes* membrane fraction amounts to 27 U mg protein^{-1} (Table 3). The K_M value for fumarate of the *H. pylori* enzyme was determined as 0.83 mM [67,68]. Taken together, the data suggest that the amount of the succinate:quinone oxidoreductase present in *H. pylori* is probably less than 10% of that found in *W. succinogenes* where the QFR amounts to approximately 2% of the membrane protein in fumarate-grown cells. However, it cannot be excluded that a considerable amount of enzyme activity was lost during the preparation of the *H. pylori* cell lysates.

Fumarate reduction activity was also determined by ^1H nuclear magnetic resonance spectroscopy recording the increase of the succinate concentration after addition of fumarate to a *H. pylori* lysate [67]. Although an electron donor for fumarate reduction was not added, a specific activity of 2.4 U mg protein^{-1} was determined which significantly exceeds the values measured with artificial substrates (Table 3). In similar experiments the specific fumarate reductase activity in a *C. jejuni* cell lysate was only 0.016 U mg protein^{-1}, and the K_M value of fumarate reductase for fumarate was 1.9 mM [37].

6. SQR and the citric acid cycle in aerobic ε-proteobacteria

Cells of *H. pylori* were reported to consume O_2 in the presence of glucose, pyruvate, ethanol, D-lactate, fumarate and succinate [69]. The molar ratios O_2 per substrate indicated that the substrates were not fully converted to CO_2. The conversion of succinate to CO_2 would require a ratio of 3.5, whereas the experimentally determined ratio was 1.5 [20] or 2 [69]. A ratio of 1.5 is consistent with the oxidation of succinate to acetate and 2 CO_2. The ratios measured with lactate or pyruvate were above those expected for conversion to acetate, but below that of complete oxidation to CO_2 [69]. Acetate oxidation by O_2 was

not reported to occur in *H. pylori*. Taken together, the data suggest that acetate is a major product of *H. pylori* respiration with the substrates indicated above, and that the succinate:quinone oxidoreductase of *H. pylori* seems to serve in succinate oxidation to acetate.

The presence of all enzymes involved in the catalysis of the citric acid cycle is regarded to be indicative that the succinate:quinone oxidoreductase predominantly catalyses succinate oxidation rather than fumarate reduction. Recently, in the genome of *H. pylori* the genes of enzymes were discovered that would make up a modified citric acid cycle. Oxidation of 2-oxoglutarate seems to be catalysed by a 2-oxoglutarate:acceptor oxidoreductase that probably uses ferredoxin as electron acceptor instead of NAD [70]. A malate:quinone oxidoreductase was characterised that unidirectionally converts malate to oxaloacetate [71]. The conversion of succinyl-CoA to succinate might be catalysed by succinyl-CoA:acetoacetyl-CoA transferase [72]. Genes predicted to encode citrate synthase, aconitase, isocitrate dehydrogenase and fumarase were found on the *H. pylori* genome [23]. The modifications noted above argue for a citric acid cycle despite the absence of genes typically encoding 2-oxoglutarate dehydrogenase, succinate thiokinase or NAD-dependent malate dehydrogenase. Parkhill et al. [25] proposed a complete citric acid cycle for *C. jejuni* by analysing the genome sequence.

7. Inactivation of *frd* genes

Deletion of the *frdCAB* operon in the genome of *W. succinogenes* resulted in a mutant that did not grow by fumarate respiration [40]. Cells grown at the expense of nitrate respiration did not contain fumarate reductase activity measured with benzyl viologen radical as electron donor. In the presence of excess fumarate, the deletion strain consumed only a small amount of fumarate for biosynthesis [73]. The results indicate that *W. succinogenes* synthesises only one enzyme that catalyses fumarate reduction. The insertional inactivation of the *frdA* gene in *H. pylori* similarly resulted in a strain that lacked fumarate reductase activity [41]. Growth of the mutant in complex medium under microaerobic conditions was only slightly affected suggesting a non-essential role of FrdA. On the other hand, the *frdA* mutant of *H. pylori* was found not to be able to colonise the stomach of mice [74]. The reason for this is not known but the result suggests that FrdA is essential for the survival of *H. pylori* in the gastric mucosa. The enzyme can therefore be regarded as a factor of pathogenicity.

8. Inhibition of *frd* gene products

Several species of the genera *Helicobacter* and *Campylobacter* are known as pathogens. The succinate:quinone oxidoreductases of these organisms are being discussed as potential drug targets, especially in the treatment of *H. pylori* infection. Mendz et al. [68] reported that several anthelminthics (oxantel, thiabendazole, morantel, see Fig. 8) affected the activity of *H. pylori* fumarate reduction in cell lysates or membrane fractions. These authors showed that oxantel is a competitive inhibitor of *H. pylori* succinate:quinone oxidoreductase. In the presence of 0.1 mM oxantel the K_M for fumarate was raised from 0.83 mM to an apparent K_M of 2.20 mM while the maximal specific activity was not altered. All three

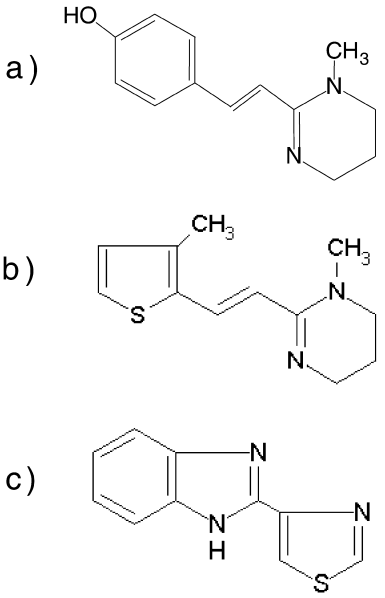

Fig. 8. Compounds suggested [37,68] to be inhibitors of succinate:quinone oxidoreductases from ε-proteobacteria: (a) oxantel, (b) morantel and (c) thiabendazole.

anthelminthics impaired cell growth in liquid cultures but the minimal inhibitory and minimal bactericidal concentrations were in the millimolar range which is not suited for therapeutic treatment. Since the succinate:quinone oxidoreductase is assumed not to be essential for growth under the conditions used for the inhibitor studies (see Section 7), it is likely that the antiparasites affected further targets beside fumarate reduction. Similar inhibitor studies were carried out with *C. jejuni* and results comparable to those with *H. pylori* were obtained [37].

9. Conclusion

Succinate:quinone oxidoreductases are versatile enzymes that can function in either the oxidation of succinate or the reduction of fumarate. Although the predicted products of ε-proteobacterial *frd* genes are very similar, the function of the corresponding enzymes may differ. Certain ε-proteobacteria grow anaerobically at the expense of fumarate respiration. In this case, fumarate reduction is catalysed at high rates by a QFR. In organisms that grow only under microoxic conditions like *H. pylori* a terminal cytochrome oxidase appears obligatory. Apparently *H. pylori*, like *C. jejuni*, cannot grow by fumarate respiration in the absence of oxygen. The low specific activity of the succinate:quinone oxidoreductase of these organisms further argues against its involvement in a fumarate respiration pathway. Therefore, it is likely that this enzyme predominantly functions as a SQR. It should be kept in mind, however, that such an enzyme might be used as a QFR in the natural habitats of *H. pylori* or *Campylobacter* spp.

Acknowledgements

C.R.D.L. thanks Hartmut Michel for generous support. Both authors are grateful to Achim Kröger for stimulating discussions and continuous support.

References

[1] P. Vandamme, E. Falsen, R. Rossau, B. Hoste, P. Segers, R. Tytgat, J. DeLey, Int. J. Syst. Bacteriol. 41 (1991) 88–103.
[2] T.M. Wassenaar, D.G. Newell, in: M. Dworkin et al. (Eds.), The Prokaryotes: An Evolving Electronic Resource for the Microbiological Community, 3rd edn., Springer-Verlag, New York, 2000.
[3] F.C. Tenover, C.L. Fennell, in: A. Balows et al. (Eds.), The Prokaryotes, 2nd edn., Springer-Verlag, New York, 1991.
[4] J. Simon, R. Gross, O. Klimmek, A. Kröger, in: M. Dworkin et al. (Eds.), The Prokaryotes: An Evolving Electronic Resource for the Microbiological Community, 3rd edn., Springer-Verlag, New York, 2000.
[5] H. Scholz-Muramatsu, A. Neumann, M. Meßmer, E. Moore, G. Diekert, Arch. Microbiol. 163 (1995) 48–56.
[6] W. Schumacher, P.M.H. Kroneck, N. Pfennig, Arch. Microbiol. 158 (1992) 287–293.
[7] M.L. Blaser, J. Infect. Dis. 176 (1997) S103–S105.
[8] L.-E. Hansson, World J. Surg. 24 (2000) 315–320.
[9] H. Kuniyasu, W. Yasui, H. Yokozaki, E. Tahara, Langenbeck's Arch. Surg. 385 (2000) 69–74.
[10] K. Finster, W. Liesack, B.J. Tindall, Int. J. Syst. Bacteriol. 47 (1997) 1212–1217.
[11] J.F. Stolz, D.J. Ellis, J.S. Blum, D. Ahmann, D.R. Loveley, R.S. Oremland, Int. J. Syst. Bacteriol. 49 (1999) 1177–1180.
[12] N.J. Jacobs, M.J. Wolin, Biochim. Biophys. Acta 69 (1963) 18–28.
[13] M.J. Wolin, E.A. Wolin, N.J. Jacobs, J. Bacteriol. 81 (1961) 911–917.
[14] A. Kröger, S. Biel, J. Simon, R. Gross, G. Unden, C.R.D. Lancaster, Biochim. Biophys. Acta 1553 (2002) 23–38.
[15] M. Véron, A. Lenvoisé-Furet, P. Beaune, Curr. Microbiol. 6 (1981) 349–354.
[16] H. Ohta, J.C. Gottschal, FEMS Microbiol. Ecol. 53 (1988) 79–86.
[17] Y.H. Han, R.M. Smibert, N.R. Krieg, Int. J. Syst. Bacteriol. 41 (1991) 218–222.
[18] C.R.D. Lancaster, A. Kröger, M. Auer, H. Michel, Nature 402 (1999) 377–385.
[19] A. Marais, G.L. Mendz, S.L. Hazell, F. Megraud, Microbiol. Mol. Biol. Rev. 63 (1999) 642–674.
[20] D.J. Kelly, Adv. Microb. Physiol. 40 (1998) 137–189.
[21] P. Doig et al., Microbiol. Mol. Biol. Rev. 63 (1999) 675–707.
[22] D.J. Kelly, J. Appl. Microbiol. 90 (2001) S16–S24.
[23] J.-F. Tomb et al., Nature 388 (1997) 539–547.
[24] R.A. Alm et al., Nature 397 (1999) 176–180.
[25] J. Parkhill et al., Nature 403 (2000) 665–668.
[26] C. Hägerhäll, Biochim. Biophys. Acta 1320 (1997) 107–141.
[27] E. Lemma, C. Hägerhäll, V. Geisler, U. Brandt, G. von Jagow, A. Kröger, Biochim. Biophys. Acta 1059 (1991) 281–285.
[28] P. Mitchell, Science 206 (1979) 1148–1159.
[29] J. Schirawski, G. Unden, Eur. J. Biochem. 257 (1998) 210–215.
[30] M. Schnorpfeil, I.G. Janausch, S. Biel, A. Kröger, G. Unden, Eur J. Biochem. 268 (2001) 3069–3074.
[31] A. Kröger, V. Geisler, E. Lemma, F. Theis, R. Lenger, Arch. Microbiol. 158 (1992) 311–314.

[32] M. Bronder, H. Mell, E. Stupperich, A. Kröger, Arch. Microbiol. 131 (1982) 216–223.
[33] B.C. Berks, M.D. Page, D.J. Richardson, A. Reilly, A. Cavill, F. Outen, S. Ferguson, Mol. Microbiol. 15 (1995) 319–331.
[34] F. Dross, V. Geisler, R. Lenger, F. Theis, T. Krafft, F. Fahrenholz, E. Kojro, A. Duchêne, D. Tripier, K. Juvenal, A. Kröger, Eur. J. Biochem. 206 (1992) 93–102 and 214 (1993) 949–950 (erratum).
[35] M. Bokranz, M. Gutmann, C. Körtner, E. Kojro, F. Fahrenholz, F. Lauterbach, A. Kröger, Arch. Microbiol. 156 (1991) 119–128.
[36] R. Lenger, U. Herrmann, R. Gross, J. Simon, A. Kröger, Eur. J. Biochem. 246 (1997) 646–651.
[37] M.A. Smith, G.L. Mendz, M.A. Jorgensen, S.L. Hazell, Int. J. Biochem. Cell Biol. 31 (1999) 961–975.
[38] C. Körtner, F. Lauterbach, D. Tripier, G. Unden, A. Kröger, Mol. Microbiol. 4 (1990) 855–860.
[39] F. Lauterbach, C. Körtner, S.P.J. Albracht, G. Unden, A. Kröger, Arch. Microbiol. 154 (1990) 386–393.
[40] J. Simon, R. Gross, M. Ringel, E. Schmidt, A. Kröger, Eur. J. Biochem. 251 (1998) 418–426.
[41] Z. Ge, Q. Jiang, M.S. Kalisiak, D.E. Taylor, Gene 204 (1997) 227–434.
[42] S. Janssen, G. Schäfer, S. Anemüller, R. Moll, J. Bacteriol. 179 (1997) 5560–5569.
[43] C.M. Gomes, R.S. Lemos, M. Teixeira, A. Kletzin, H. Huber, K.O. Stetter, G. Schäfer, S. Anemüller, Biochim. Biophys. Acta 1411 (1999) 134–141.
[44] C.R.D. Lancaster, Biochim. Biophys. Acta 1553 (2002) 1–6.
[45] G. Schäfer, S. Anemüller, R. Moll, Biochim. Biophys. Acta 1553 (2002) 57–73.
[46] R.S. Lemos, A.S. Fernandes, M.M. Pereira, C.M. Gomes, M. Teixeira, Biochim. Biophys. Acta 1553 (2002) 158–170.
[47] C.R.D. Lancaster, R. Gross, A. Haas, M. Ritter, W. Mäntele, J. Simon, A. Kröger, Proc. Natl. Acad. Sci. USA 97 (2000) 13051–13056.
[48] C.R.D. Lancaster, R. Gross, J. Simon, Eur. J. Biochem. 268 (2001) 1820–1827.
[49] C.R.D. Lancaster, in: C. Hunte, H. Schägger, G. von Jagow (Eds.), Membrane Protein Purification and Crystallization: A Practical Guide, 2nd edn., Academic Press, San Diego, CA, 2001.
[50] C.R.D. Lancaster, A. Kröger, Biochim. Biophys. Acta 1459 (2000) 422–431.
[51] W.C. Kenny, A. Kröger, FEBS Lett. 73 (1977) 239–243.
[52] C.R.D. Lancaster, FEBS Lett. 504 (2001) 133–141.
[53] C. Hägerhäll, L. Hederstedt, FEBS Lett. 389 (1996) 25–31.
[54] H. Luecke, B. Schobert, H.T. Richter, J.-P. Cartailler, J.K. Lanyi, J. Mol. Biol. 291 (1999) 899–911.
[55] J. Vonck, Biochemistry 35 (1996) 5870–5878.
[56] D. Xia, C.A. Yu, H. Kim, J.Z. Xian, A.M. Kachurin, L. Zhang, L. Yu, J. Deisenhofer, Science 277 (1997) 60–66.
[57] C.R.D. Lancaster, H. Michel, Structure 5 (1997) 1339–1359.
[58] G. Unden, S.P.J. Albracht, A. Kröger, Biochim. Biophys. Acta 767 (1984) 460–469.
[59] C.C. Page, C.C. Moser, X. Chen, P.L. Dutton, Nature 402 (1999) 47–52.
[60] A. Kröger, A. Innerhofer, Eur. J. Biochem. 69 (1976) 497–506.
[61] J.C. Salerno, Biochem. Soc. Trans. 19 (1991) 599–605.
[62] P.L. Dutton, X. Chen, C.C. Page, S. Huang, T. Ohnishi, C.C. Moser, in: G.W. Canters, E. Vijgenboom (Eds.) Biological Electron Transfer Chains: Genetics, Composition and Mode of Operation, Kluwer Academic, Dordrecht, 1998, pp. 3–8.
[63] G. Unden, H. Hackenberg, A. Kröger, Biochim. Biophys. Acta 591 (1980) 275–288.
[64] C.R.D. Lancaster, in: A. Messerschmidt, R. Huber, T. Poulos, K. Wieghardt (Eds.), Handbook of Metalloproteins, Vol. 1, J. Wiley and Sons, Chichester, 2001, pp. 379–401.
[65] S. Birkholz, U. Knipp, E. Lemma, A. Kröger, W. Opferkuch, J. Med. Microbiol. 41 (1994) 56–62.
[66] M. Chen, L.P. Andersen, L. Zhai, A. Kharazmi, FEMS Immunol. Med. Microbiol. 24 (1999) 169–174.
[67] S.M. Pitson, G.L. Mendz, S. Srinivasan, S.L. Hazell, Eur. J. Biochem. 260 (1999) 258–267.
[68] G.L. Mendz, S.L. Hazell, S. Srinivasan, Arch. Biochim. Biophys. 321 (1995) 153–159.
[69] H.T. Chang, S.W. Marcelli, A.A. Davison, P.A. Chalk, R.K. Poole, R.J. Miles, FEMS Microbiol. Lett. 129 (1995) 33–38.
[70] N.J. Hughes, C.L. Clayton, P.A. Chalk, D.J. Kelly, J. Bacteriol. 180 (1998) 1119–1128.
[71] B. Kather, K. Stingl, M.E. van der Rest, K. Altendorf, D. Molenaar, J. Bacteriol. 182 (2000) 3204–3209.
[72] I.E. Corthesy-Theulaz, G.E. Bergonzelli, H. Henry, D. Bachmann, D.F. Schorderet, A.L. Blum, L.N. Ornston, J. Biol. Chem. 272 (1997) 25659–25667.
[73] J. Simon, R. Gross, O. Klimmek, M. Ringel, A. Kröger, Arch. Microbiol. 169 (1998) 424–433.
[74] Z. Ge, Y. Feng, C.A. Dangler, S. Xu, N.S. Taylor, J.G. Fox, Microb. Pathogen. 29 (2000) 279–287.
[75] Y.H. Han, R.M. Smibert, N.R. Krieg, Can. J. Microbiol. 38 (1992) 104–110.
[76] S.W. Marcelli, H.T. Chang, T. Chapman, P.A. Chalk, R.J. Miles, R.K. Poole, FEMS Microbiol. Lett. 138 (1996) 59–64.
[77] P.S. Hoffman, T.G. Goodman, J. Bacteriol. 150 (1982) 319–326.
[78] M.D. Collins, F. Widdel, Syst. Appl. Microbiol. 8 (1986) 8–18.
[79] J. Lorenzen, S. Steinwachs, G. Unden, Arch. Microbiol. 162 (1994) 277–281.
[80] J. Simon, Ph.D. Thesis, J.W. Goethe University, Frankfurt am Main, 1998.
[81] P.J. Kraulis, J. Appl. Crystallogr. 24 (1991) 946–950.
[82] R.M. Esnouf, J. Mol. Graphics Mod. 15 (1997) 132–134.
[83] E.A. Merrit, D.J. Bacon, Methods Enzymol. 277 (1997) 505–524.